Neutrinos **E**lectro-**W**eak interactions
and **S**ymmetries **(March 27, 2025)**

Experimental search for new gravity-like interaction in the submicron range by means of the small-angle neutron scattering

Masayuki Hiromoto

**Research Center for Nuclear Physics,
Osaka University**

Content

- **Target creation**
- **SANS experiment in J-PARC/MLF/BL05**
- **Analysis**

- **Target creation**

Neutron coherent scattering of nanoparticle

Differential cross section

b_{coh} : Nuclear coherent scattering length

$b_Y(q)$: Scattering length of unknown interaction

$$\frac{d\sigma_{coh}(q,R)}{d\Omega} \propto \left(b_{coh} + b_Y(q)\right)^2 \underbrace{\int_V \rho(r)\, e^{(-i\vec{q}\cdot\vec{r})} d\vec{r}}_{\text{Form factor}}$$

- ✓ Nuclear scattering is main back ground.
- ✓ Analysis of q dependence due to nanoparticle shape and structure is required.

Coherent nuclear scattering length

Data list of b_{coh} (by NIST)

H	-3.7390 ± 0.0011 fm
O	5.803 ± 0.004 fm
V	-0.555 ± 0.003 fm
Fe	9.45 ± 0.02 fm
Ni	10.3 ± 0.1 fm
^{62}Ni	-8.7 ± 0.2 fm

The element with the smallest value

T. Fujiie, Phys. Rev. Lett., vol. 132, p. 023402, Jan 2024.

How to reduce BG by nuclear scattering ?

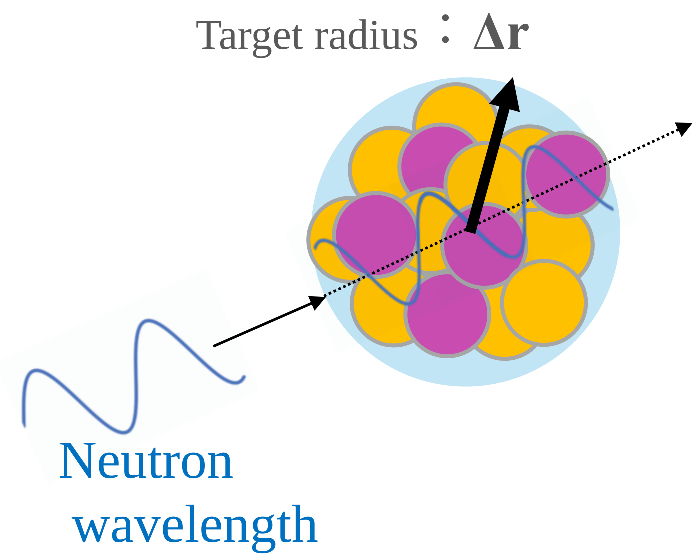

: element of (positive coh. scattering length) b_+

: element of (negative coh. scattering length) b_-

k: Mixing ratio of isotope for b_+

$$\overline{b_{coh}} = (1-k)b_+ + kb_- \approx 0$$

⇒ Mix several elements to adjust the coherent nuclear scattering length to zero.

Null matrix alloy nanoparticle

An alloy containing elements in a ratio such that $\overline{b_{coh}}$ is zero (Null matrix alloy) is used for neutron scattering holders, etc.

Change in Bragg peak of Vanadium alloys by adjusting Ni content ratio

Industrial Users Society for Neutron Application Vol.37, 2017.

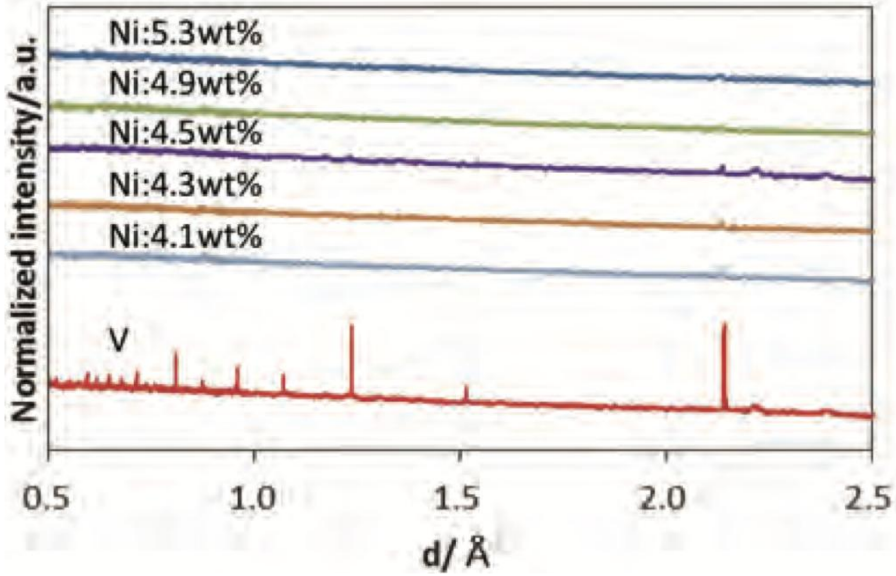

Differential cross section of spherical nanoparticle (radius=20 [nm])

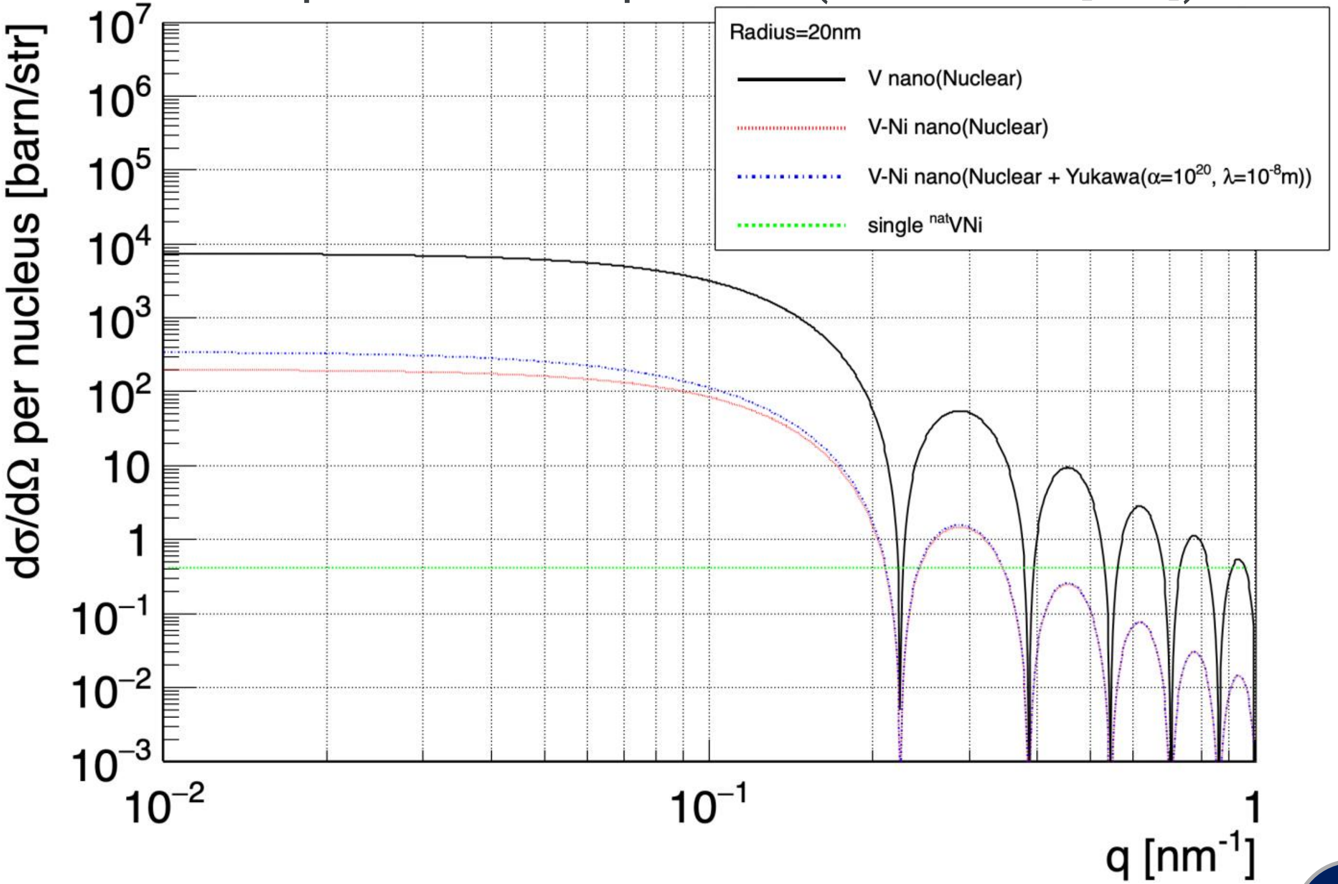

Null matrix nanoparticle creation test

There are no examples of null-matrix ($\overline{b_{coh}} \approx 0$) nanoparticles being created.
Therefore, we need to create some prototypes.

Main methods for creating nanoparticles

Ease of prototyping

Chemical precipitation	Merit	Easy to prototype in the laboratory
	Demerit	Multiple trial and error processes are required to determine conditions
Crushing	Merit	The alloy with the adjusted mixture ratio is processed into powder.
	Demerit	Possibility of contamination from equipment
Vapor phase	Merit	The main contamination depends on the ratio and purity of the raw materials.
	Demerit	Need to prepare prototype conditions and high-purity raw powder

Prototype 1. $Ni(OH)_2$ nanoparticles

Synthesis of nickel hydroxide isotopically substituted with ^{62}Ni

Data list of b_{coh} (by NIST)	
H	−3.7390(11) fm
O	5.803(4) fm
Ni	10.3(1) fm
^{62}Ni	−8.7(2) fm

When mixed in the following ratio:

$$^{62}\mathrm{Ni(OH)_2} : \mathrm{Ni(OH)_2} = 0.24 : 0.76$$

$$\rightarrow \overline{b_{coh}} = -0.012 \text{ fm}$$

Synthesis process of $Ni(OH)_2$ nanoparticles

Journal of Physics: Conference Series 741 (2016) 012194

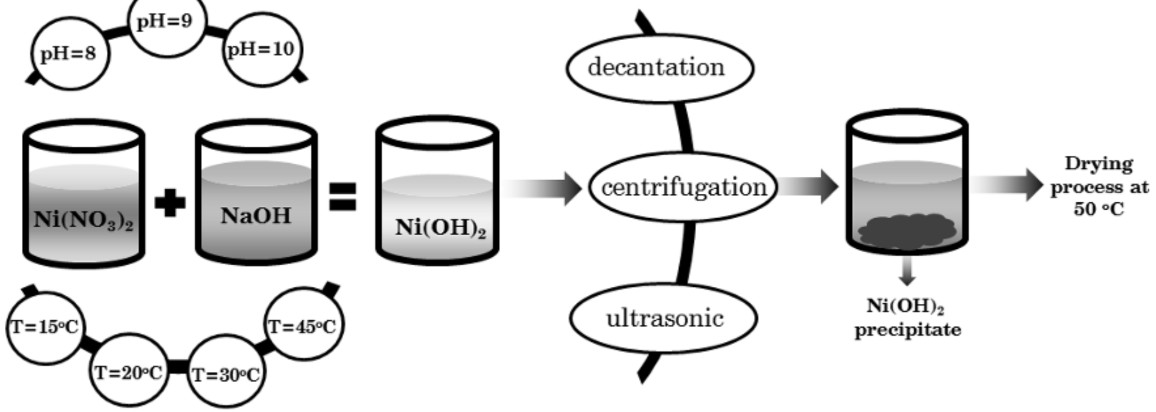

Trial $Ni(OH)_2$ colloidal solution

However, ,

The substance was deemed hazardous for use in experiments.

Other substances that can be chemically synthesized also fell into this category.

Prototype 2. Crushing of V-Ni alloy

Alloy foil with adjusted elemental mixture ratio is crushed and processed into nanoparticles

The raw material V-Ni alloy foil

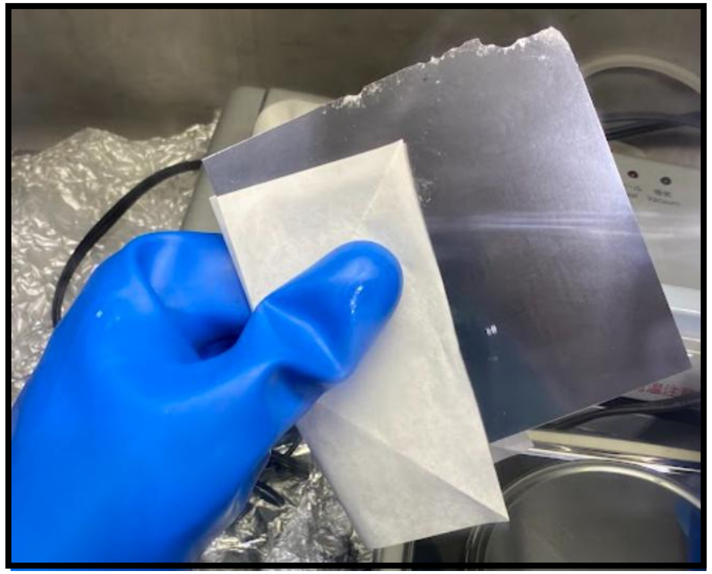

Ratio of detected elements in the V-Ni alloy

	b_{coh} [fm]	wt%
V	−0.555(3)	Bal.
Ni	10.3(1)	4.85
Al	3.449(5)	0.002
Si	4.15071(22)	0.016
Fe	9.45(2)	0.002
Mo	6.715(20)	0.001
C	6.6484(13)	0.008
O	5.805(4)	0.015
N	9.36(2)	0.013

Calculated the average coherent scattering length

$$\overline{b_{coh}} = -0.03 \text{ fm}$$

Prototype 2. Crushing of V-Ni alloy

schematic of jet mill

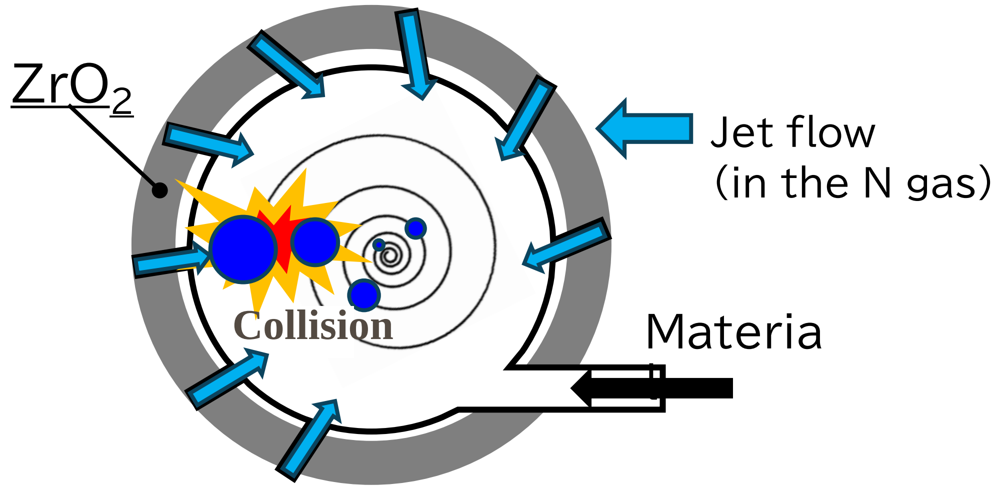

Feature of jet mill:

- The raw materials are crushed by colliding with each other.
- Contamination is minimized among all crushing methods.

SEM image of the powder after crushing

In the case of pure vanadium material

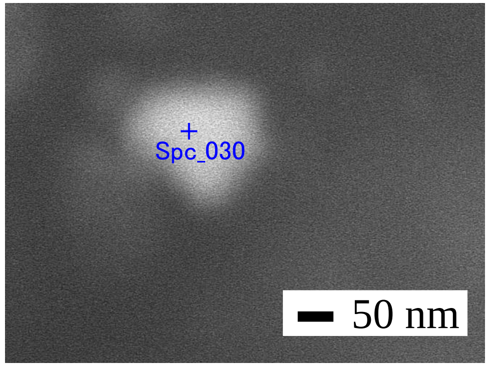

In the case of V-Ni alloy material

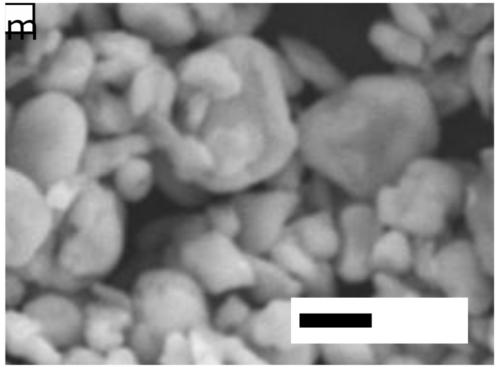

Elements detected in V-Ni powder (by EDS analysis)

$b_{coh} = 7.16(3)$ fm

	V	Ni	Zr
V-Ni powder	67.5 wt%	3.3 wt%	29.1 wt%

⇒ When V-Ni alloy is used as raw material, the processing time is long and contamination (ZrO_2) occurs from the equipment.

Prototype 3. RF thermal method

RF thermal plasma creation process

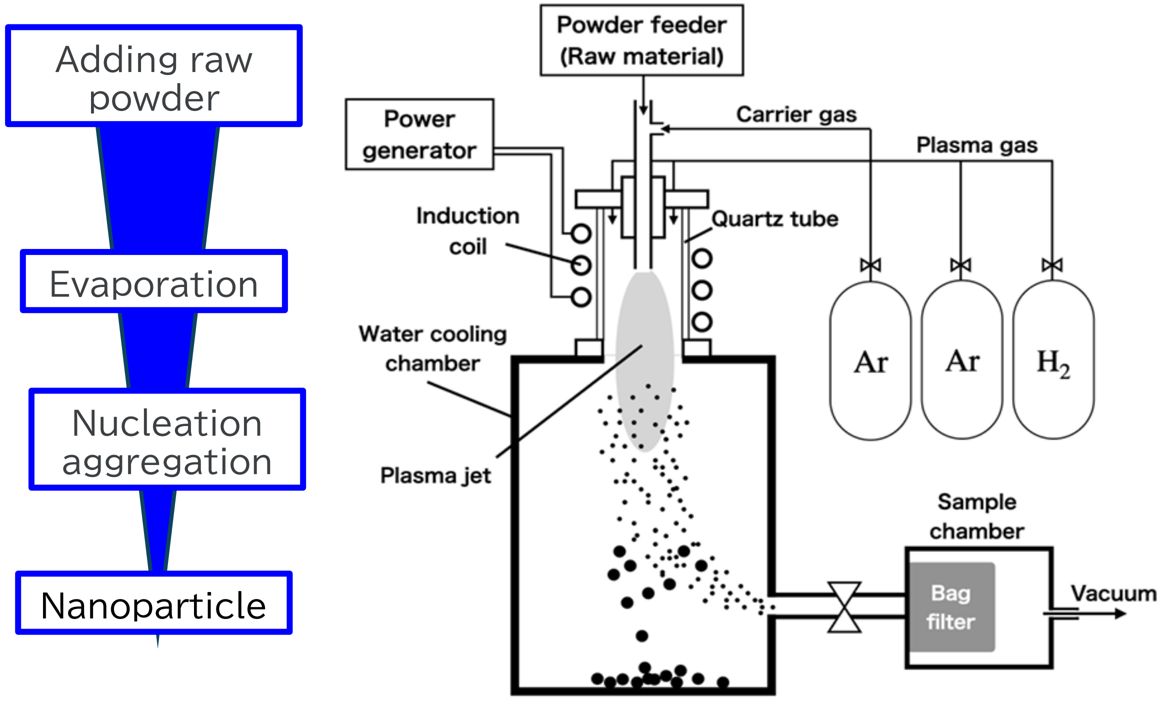

Features:

✓ No contamination from electrodes etc. occurs during the evaporation process
⇒ Contamination from equipment can be reduced

✓ Alloy nanoparticles can be created by mixing different raw powders (±0.5 wt%)

✓ Using Ar and H gas as the plasma gas prevents oxidation of metal nanoparticles

Prototype V-Ni alloy nanoparticles and pure V nanoparticles

Prototype 3. RF thermal method

SEM image of
created nanoparticles

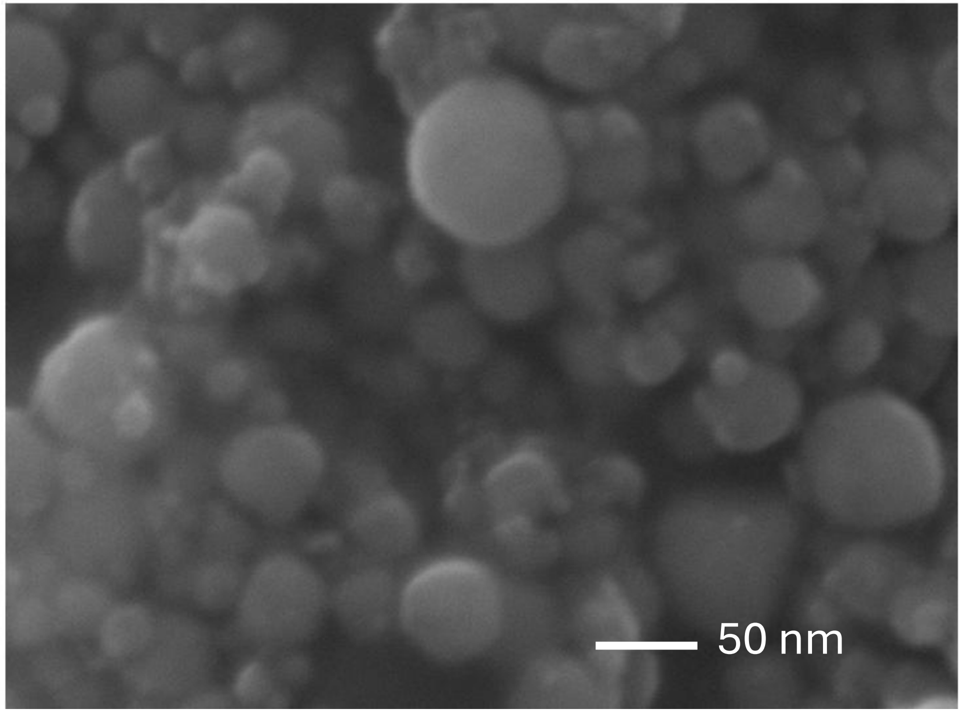

Particle size distribution

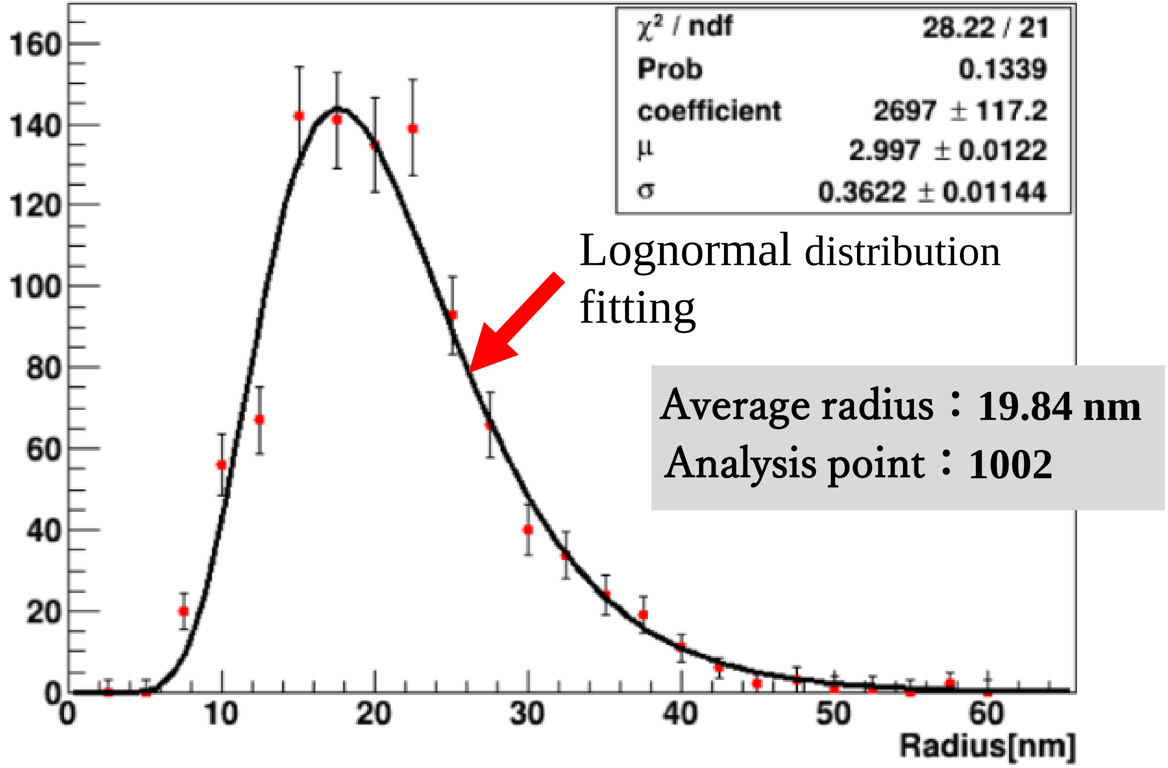

Prototype 3. RF thermal method

Mass% of elements detected in nanoparticles

C：SEM-EDS
O： HORIBA EMGA-930 (Infrared absorption method)
Metal element：ICP-AES

	C	O	B	Mg	Al	Si	Ca	Ti	V	Cr	Mn	Fe	Ni	Zn	Zr
V nanoparticle	0.68	6.15	0.0175	0.0026	0.0088	0.043	0.0036	0.001	92.97	0.028	0.0017	0.084	-	0.0088	-
V-Ni nanoparticle (@Ni = 1.9 wt%)	0.58	11.4	0.0043	0.0034	0.0079	0.040	0.0049	0.001	85.46	0.024	0.0014	0.074	2.378	0.0139	-
V-Ni nanoparticle (@Ni = 5.8 wt%)		13.4	-	0.0017	0.0273	0.042	0.0010	0.004	80.55	0.011	0.0153	0.047	5.477	0.004	0.0018

Calculated nuclear scattering length

Contamination detected in commercial products: Fe > 27wt%

	Created V nanoparticle	Created V-Ni nanoparticle	Manufacture V nanoparticle
b_{coh}	0.719±0.023 fm	1.599±0.013 fm	2.898±0.314 fm
σ_{abs}	4.08 b	3.52 b	-
σ_{inc}	4.93 b	3.70 b	-

"Created V nanoparticles" have a nuclear scattering length comparable to that of natural V (-0.555(3) fm)

- **SANS experiment in J-PARC/MLF/BL05**

Target cell

The V nanoparticles were sealed in a cell in Ar gas using a vacuum glove box to prevent contamination by oxidation.

- Oxygen concentration: **0.0±0.1 wt%**
- Dew point：< **-30 ℃dq**

Airtight holder

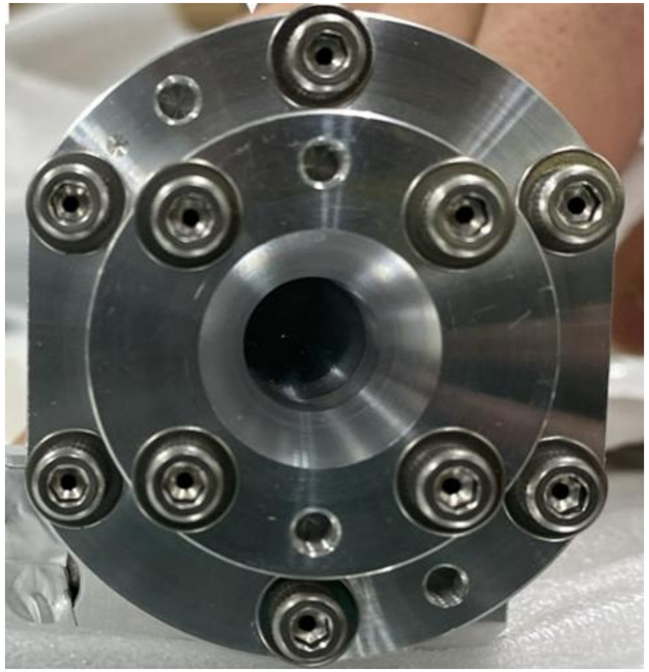

V nanopowder packed in a holder

- Filling volume：15.6 mg
- Window material：V-Ni foil (250 mmt ×2)

J-PARC/MLF/BL05/Low divergence beam brach

MLF(Material and Life Science Facility)

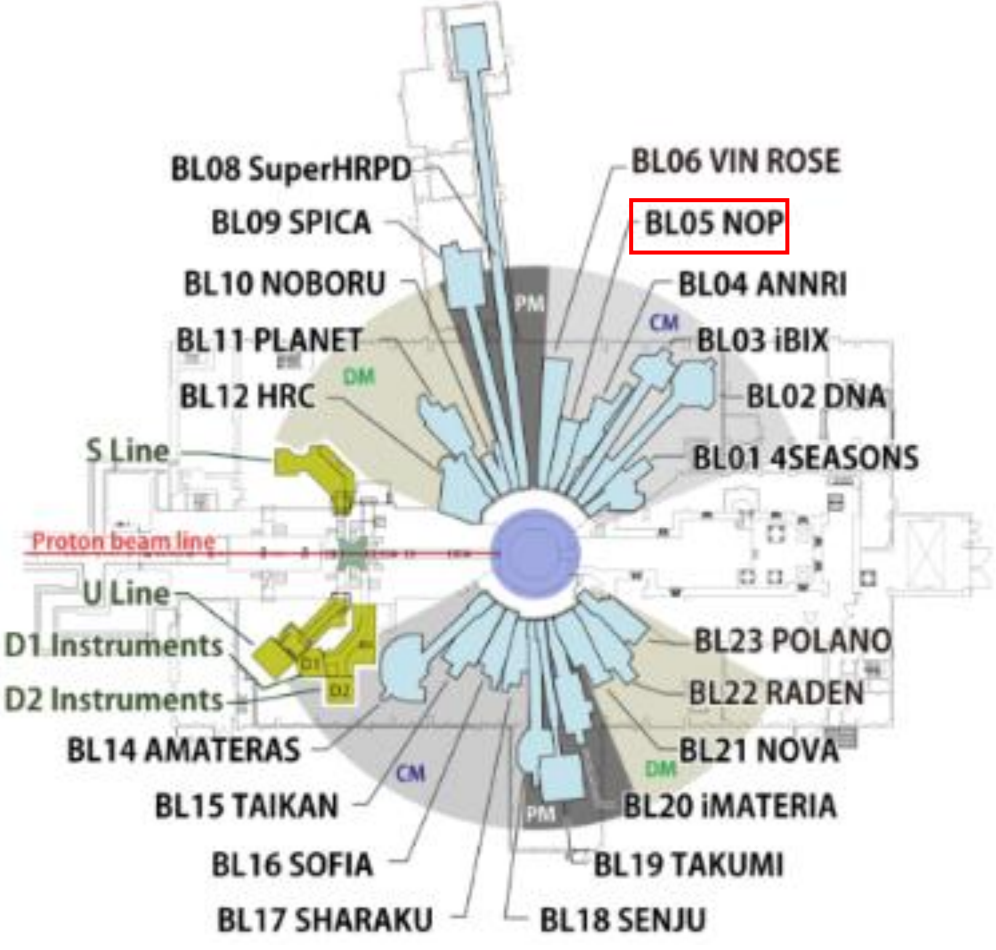

BL05 beam line

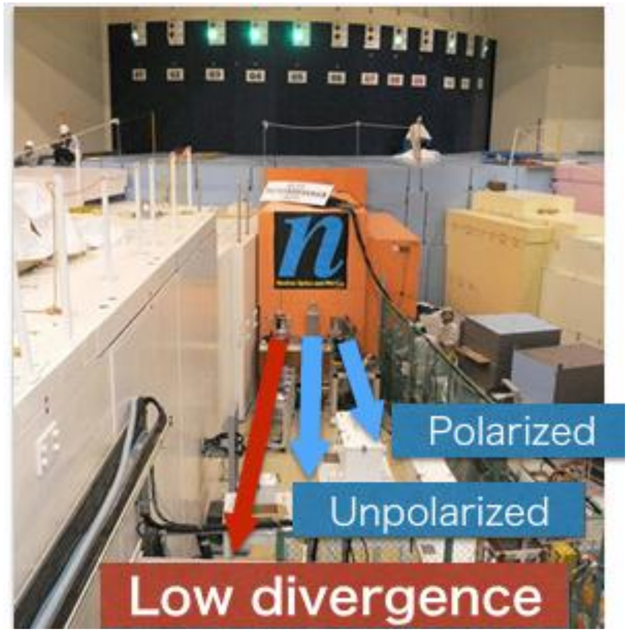

Primary beam energy：30 GeV
Proto bema power：750 kW(2023/06/15)
Pulse repetition rate：25 Hz
Neutron source：Mercury target
Average neutron energy：4 meV
Beam divergence：0.23 × 0.23 mrad

SANS experiment set up

The position and time information of the scattered neutrons are measured.

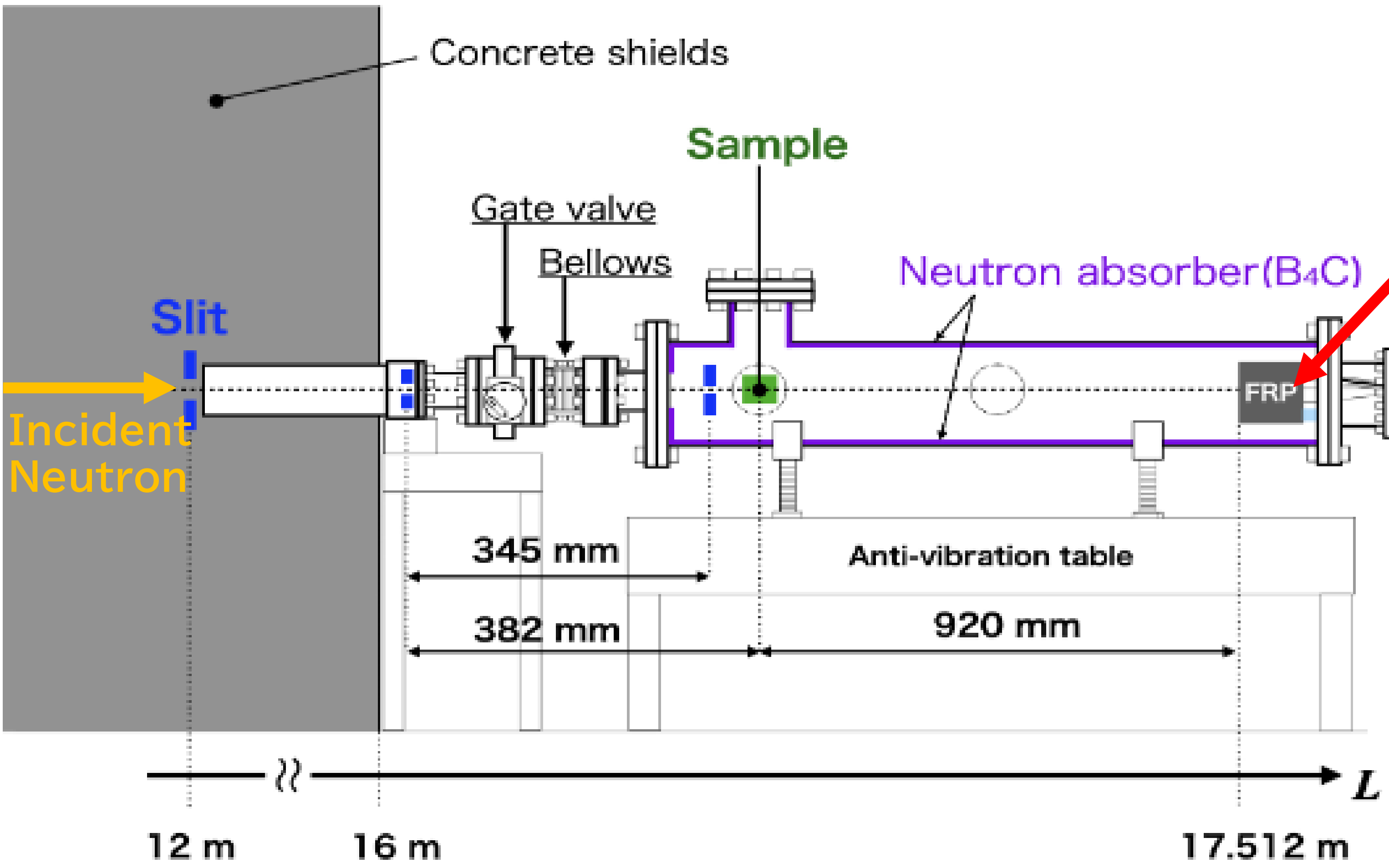

Neutron detector(FRP)

Position resolution：0.3 mm
Neutron scintillator：$^6LiF/ZnS$
PMT：Hamamatsu H12700

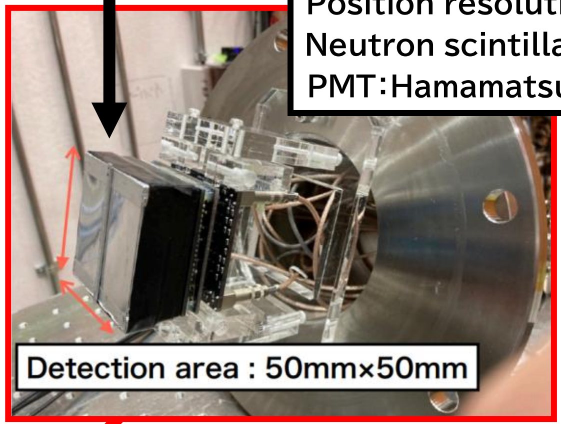

A detector that can be used in a vacuum has been constructed by Dr. Nakabe of JAWA.

R. Nakabe, Master's thesis, Nagoya University, (2020).

Incident beam profile(Line-slit)

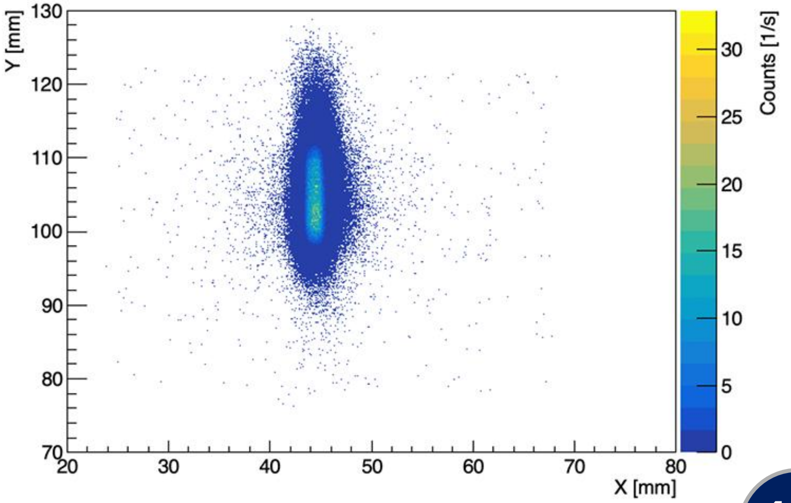

➢ Analysis

Particle size analysis of V nanoparticle

The SANS measurements are compared with SAXS (Small Angle X-ray Scattering) measurements to analyze the q dependence on particle size and shape.

Differential cross section of SANS

Form factor & Particle size

$$\frac{d\sigma_{\mathrm{SANS}}(q)}{d\Omega} = \{b_{coh} + b_Y(q)\}^2 \boxed{\int N(R) \left| \int \rho(r) exp(iqr) dV \right|^2 dR}$$

Differential cross section of SAXS

$$\frac{d\sigma_{\mathrm{SAXS}}(q)}{d\Omega} = \{b_{\mathrm{E}}\}^2 \boxed{\int N(R) \left| \int \rho(r) exp(iqr) dV \right|^2 dR}$$

b_{E} : X-ray scattering length
(X-ray scattering factor)

The q distribution is described by particle size and shape, which is the same as in SANS

q-distribution analysis of SAXS data

SAXS was performed at Aichi-SR (BL8S3) to measure the q distribution of V nanoparticles.

Camera length	6365.38 [mm]
X-ray energy	8.2 [keV]
Beam size	1.0×0.5 [mm^2]
Photon energy	3.3×10^{10} [Photons/sec]
q range	0.02 ~ 1.0 [nm^{-1}]

V nanoparticles fixed on Kapton tape

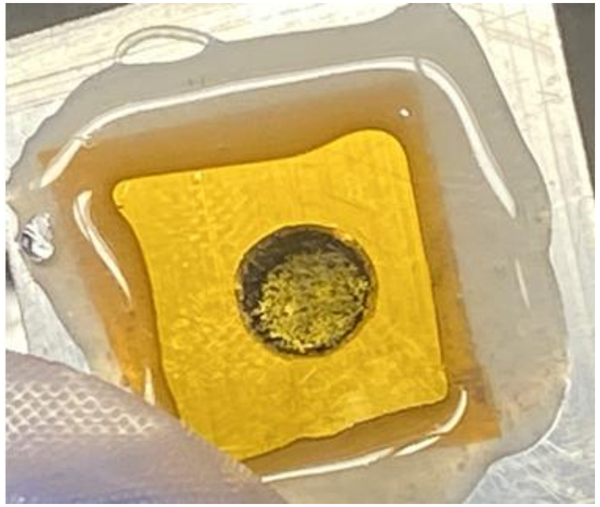

q-distribution of V nanoparticle

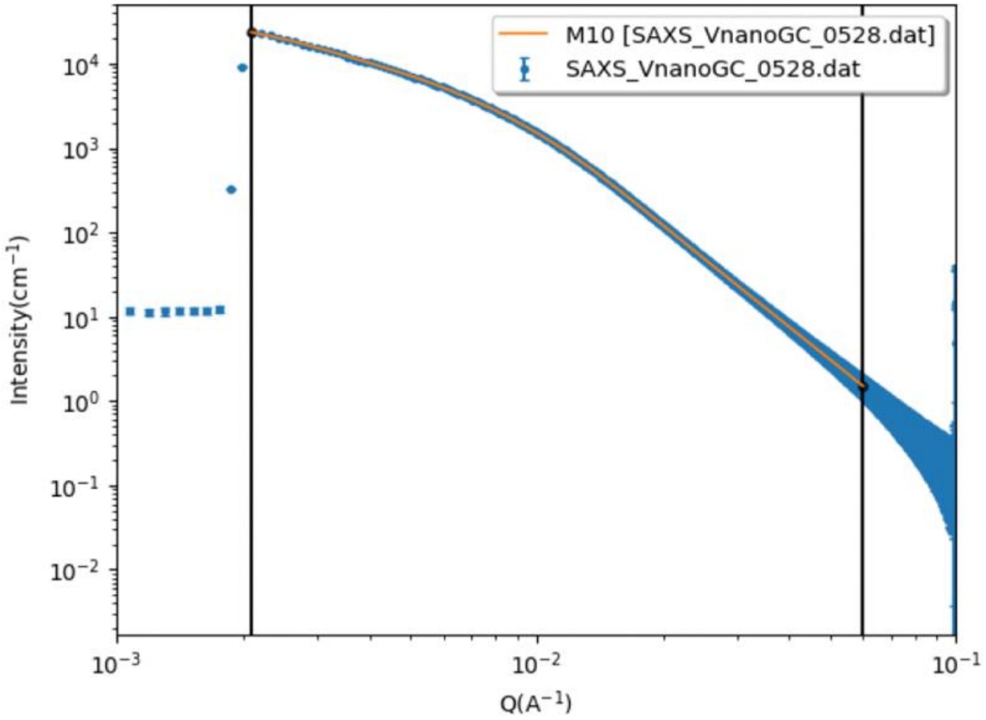

Analysis by fitting the SAXS q distribution to a particle size distribution function

Particle size data from SAXS measurement

Particle size distribution that reproduces the SAXS q distribution

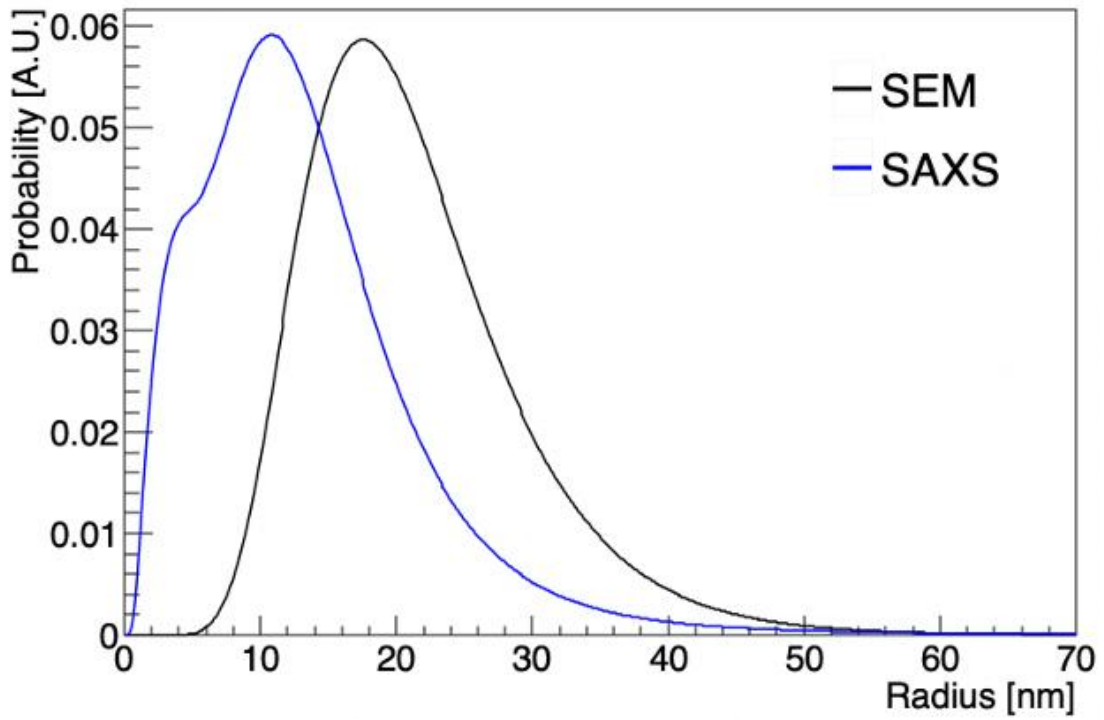

Ratio of theoretical curve from particle size to SAXS data

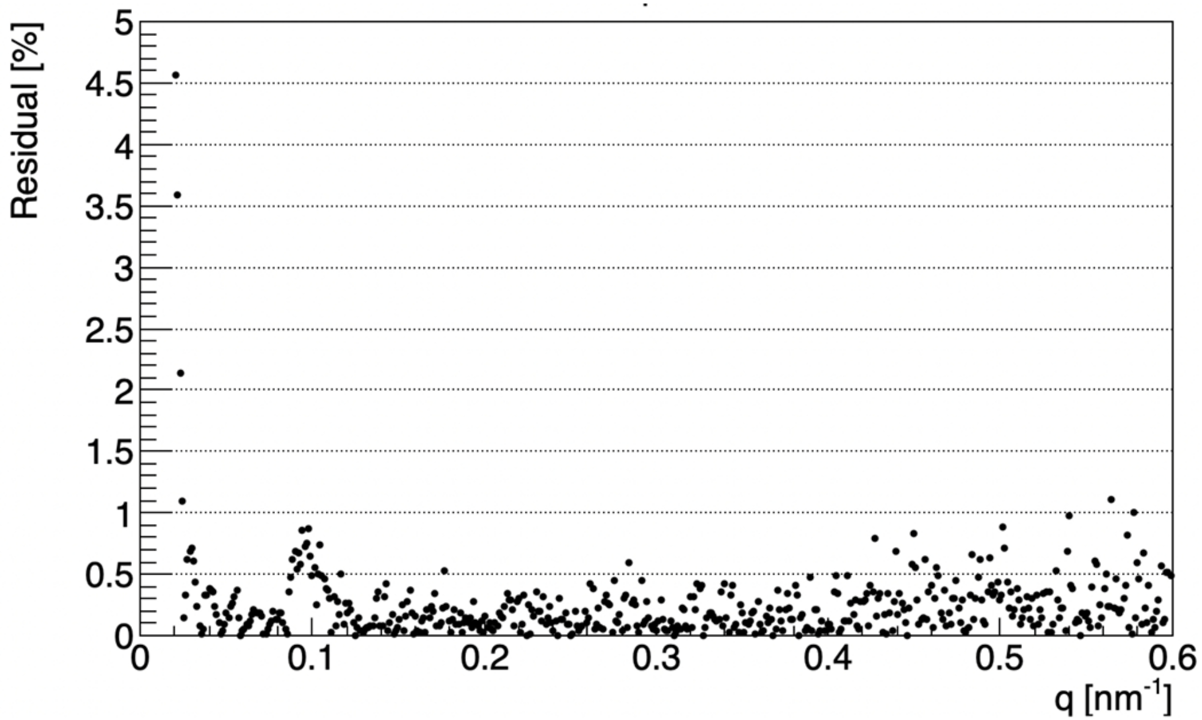

- SAXS data reveals small particles that cannot be seen by electron microscopy
- The q distribution calculated from the particle size distribution has a deviation of about 1%.
  ⇒ This is evaluated as a systematic error.

Powder packing density in a SANS cell

To determine the density of the powder in the SANS cell,
gamma ray transmittance measurements were performed.

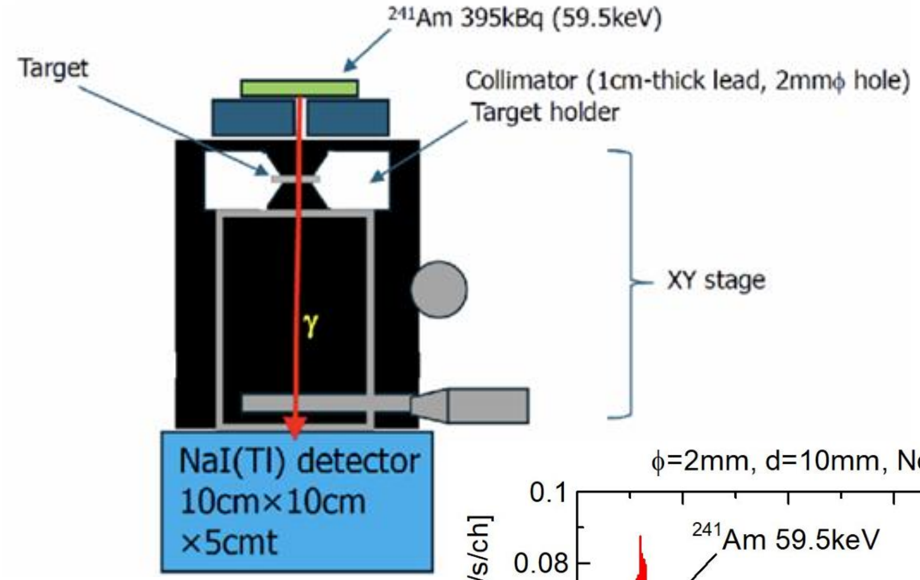

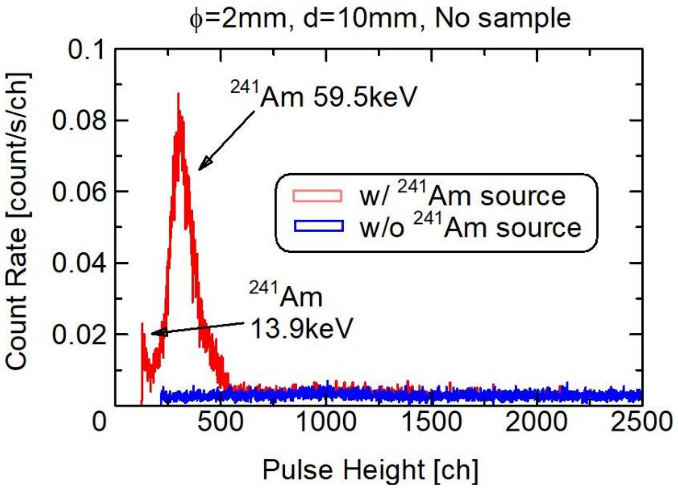

Ratio from average density of SANS cells

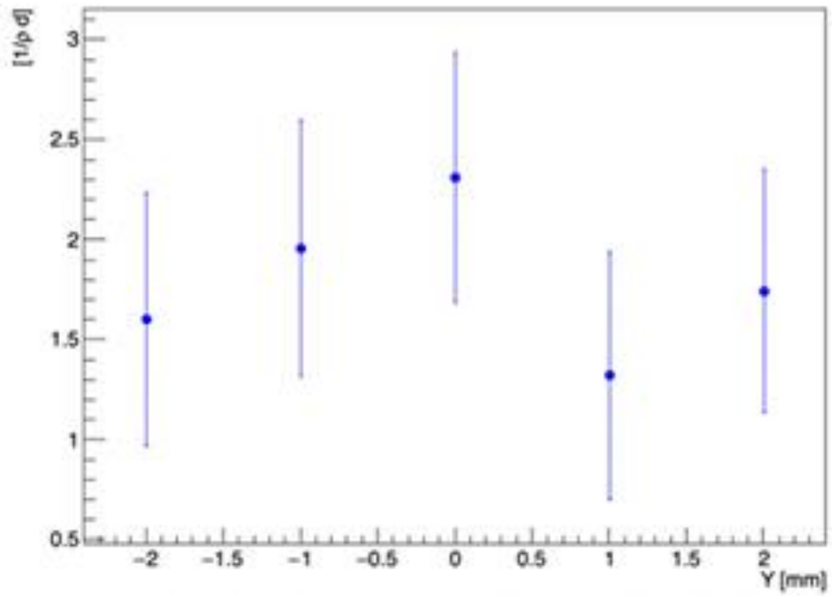

From the gamma ray transmission, it was estimated that the central density in the SANA cell was 2.31 ± 0.62 times higher than when the particles were uniformly distributed.

Effects of aggregation

When the powder is densely packed, the q distribution changes due to the aggregation of adjacent particles.

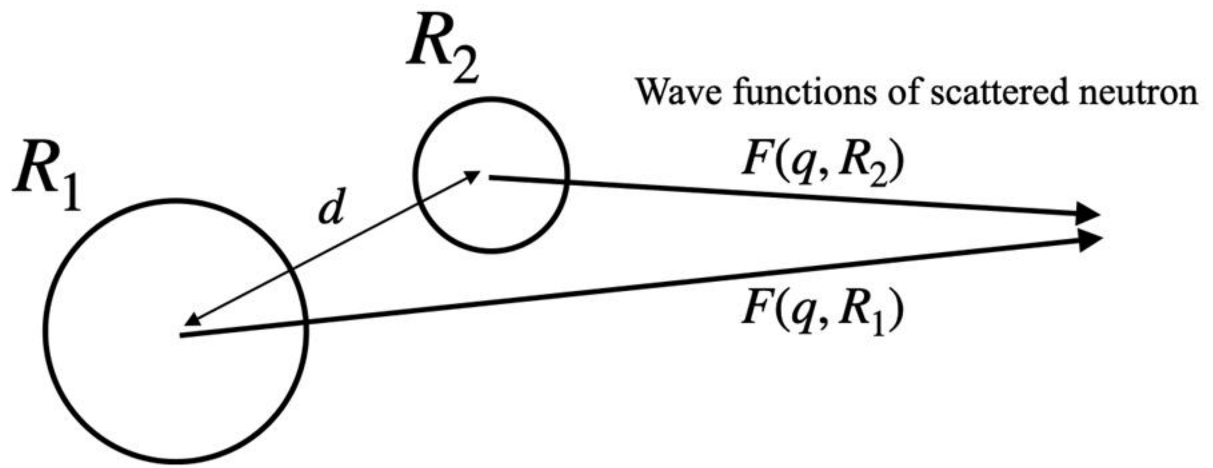

$$S'(q) = 1 + \frac{|\Sigma_i n_i F(q, R_i)|^2}{\Sigma_i |n_i F(q, R_i)|^2} \left[\frac{n_i S(q, R_i, \eta)}{\Sigma_i n_i} - 1 \right]$$

Shift in q distribution due to aggregation
(Calculations assuming average density)

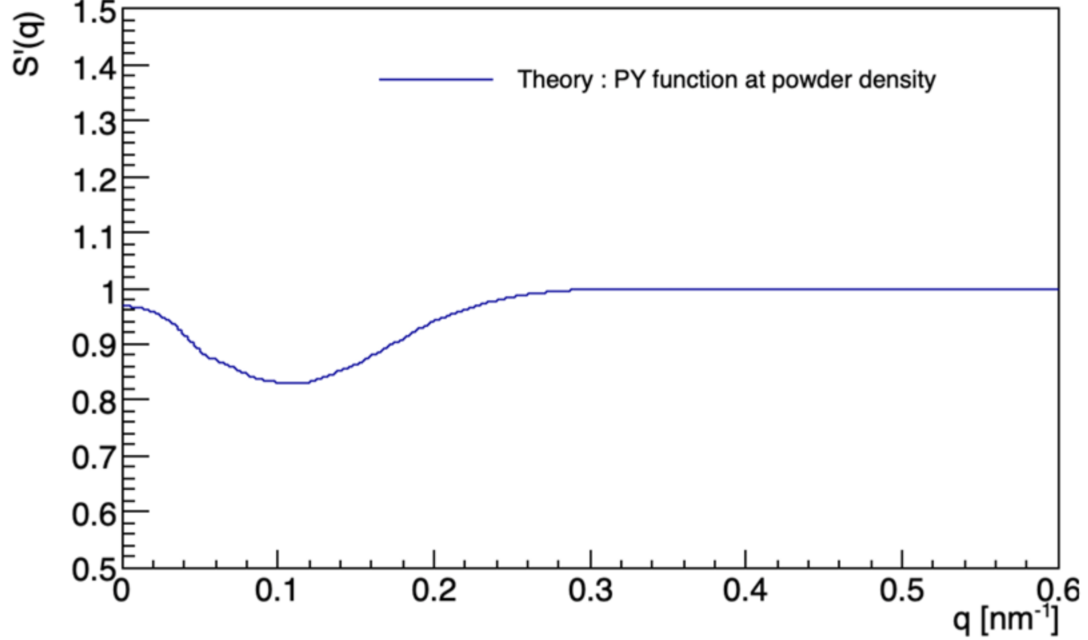

The deviation of the q distribution estimated from particle size distribution data has an effect of q < 0.3 [nm^{-1}].

Ratio from average density estimated from scattering intensity

Fitting the q-distribution of nuclear scattering simulated
by Monte Carlo with average density

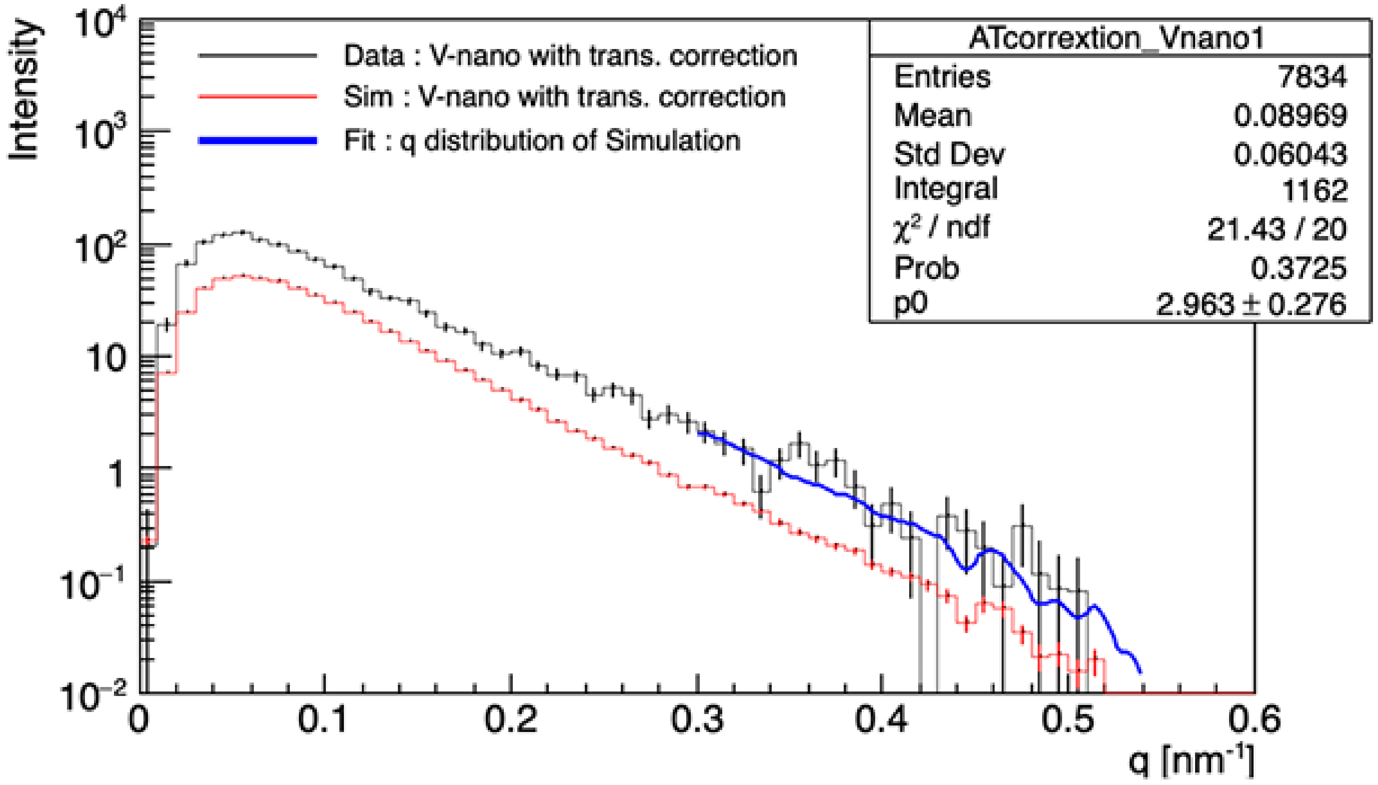

As a result, the ratio from the average density is 2.963 ± 0.276(9.3%).

Comparison with MC simulation using effective density

The results are compared with the results of simulating only nuclear scattering.

Effective density:2.963×0.263(9.3%)

Comparison of q distribution

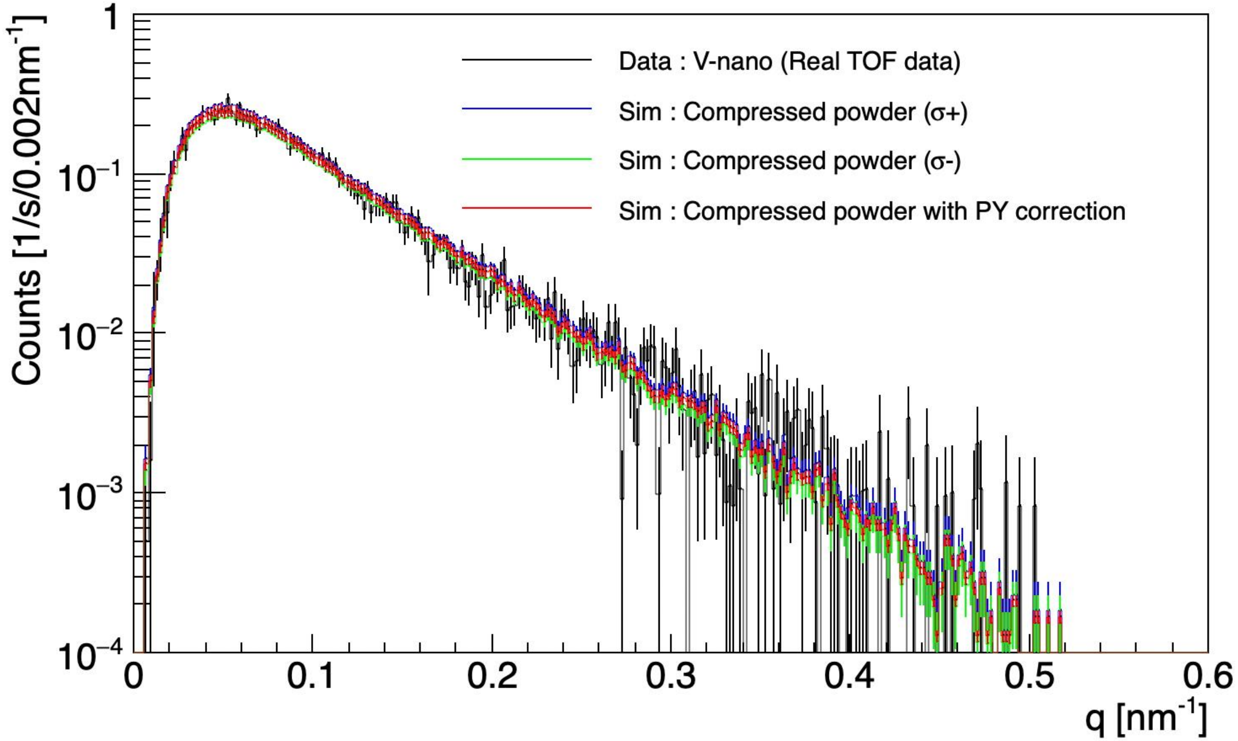

Comparison of neutron transmittance

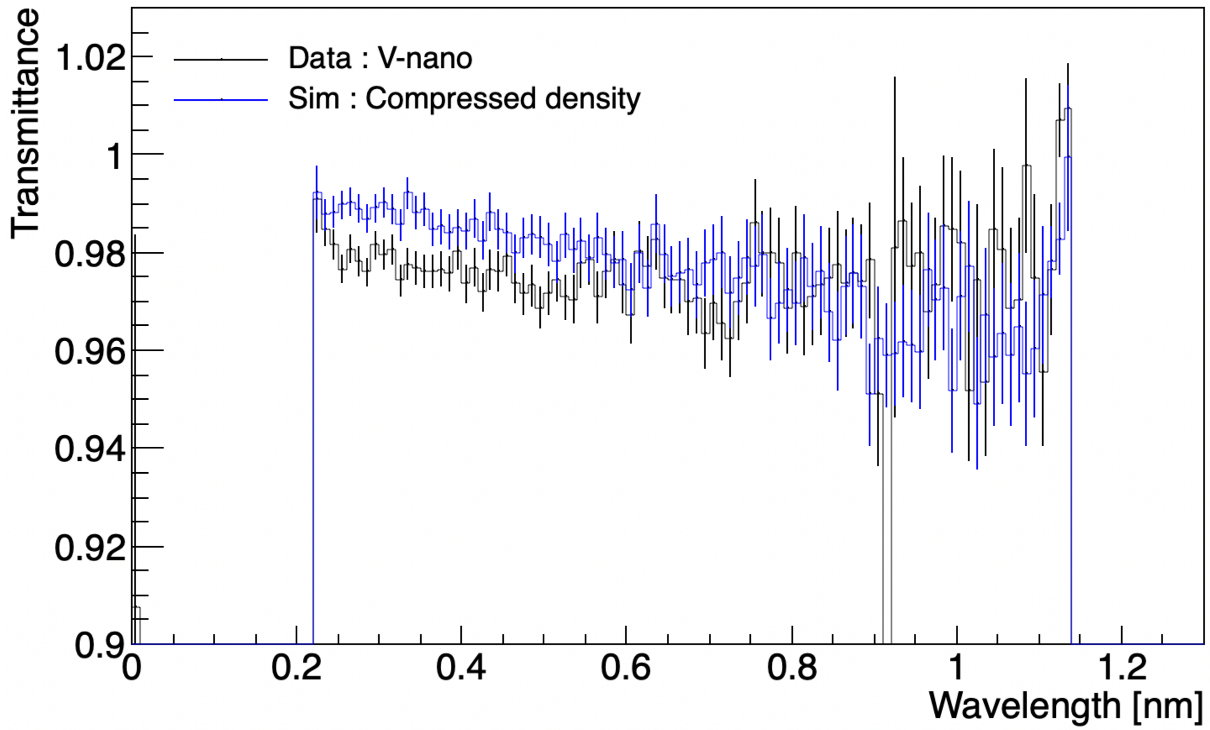

- The systematic error of the simulation is an effective density error of 9.3%.

Method for evaluating Yukawa interactions

C_{Data} and C_{Sim} : Solid angle of the detector

- Scattering intensity of data

q dependence of Yukawa interaction

$$I_{\mathrm{Data}}(\Omega, R, q) = C_{\mathrm{Data}}(\Omega) T(\lambda) \rho_{\mathrm{powder}} d * \left[S'(q) \int_R n(R) \frac{\left[V(R)\rho_{atom}(b_{\mathrm{coh(N)}} + b_{\mathrm{coh(EM)}}(q) + b_{\mathrm{Y}}(q))\right]^2}{N_{\mathrm{atom}}(R)} F(q,R)^2 dR + \sigma_{\mathrm{inc}} + \sigma_{\mathrm{diff}} \right] * \varepsilon(\lambda) I_{\mathrm{in}}(\lambda) + \mathrm{BG}(\lambda)$$

- Simulation (Only nuclear scattering)

$$I_{\mathrm{Sim}}(\Omega, R, q) = C_{\mathrm{Sim}}(\Omega) T(\lambda) \rho_{\mathrm{powder}} d * \left[S'(q) \int_R n(R) \frac{\left[V(R)\rho_{\mathrm{atoms}} b_{\mathrm{coh(N)}}\right]^2}{N_{\mathrm{atom}}(R)} F(q,R)^2 dR + \sigma_{\mathrm{inc}} + \sigma_{\mathrm{diff}} \right] * \varepsilon(\lambda) I_{\mathrm{in}}(\lambda)$$

In the case of, $\sigma_{coh} \gg \sigma_{EM}$ and $b_N \gg b_Y(q)$

$$R(q) = \frac{I_{Data}(\Omega, R, q)}{I_{Sim}(\Omega, R, q)} \approx \left[1 + \frac{2b_Y(q)}{b_{coh}}\right] \times P_{const}$$

Evaluation of q-dependence of Yukawa interaction

The upper limit is determined by fitting the magnitude of the q-dependence of the Yukawa interaction to R(q).

$$R(q) = \left[1 + P_\alpha \frac{2b_Y(q)}{b_{coh}}\right]$$

P_α : Fit parameter

Ratio of SANS data and Simulation(Nuclear)

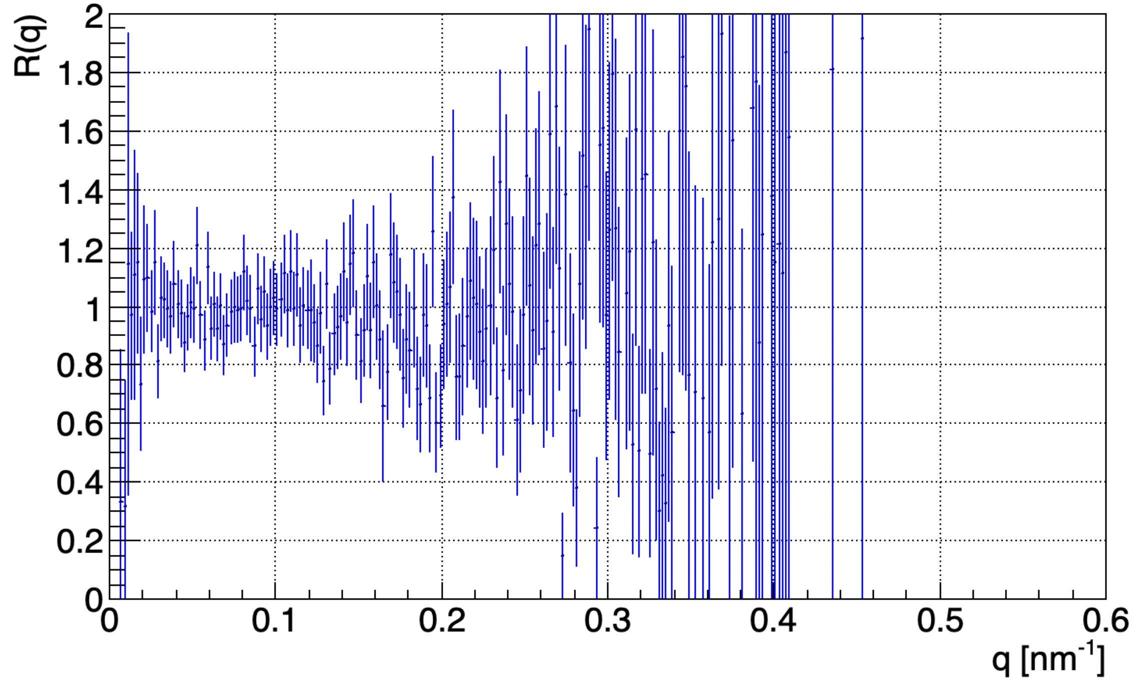

q dependence of Yukawa interaction ($\frac{2b_Y(q)}{b_{coh}}$)

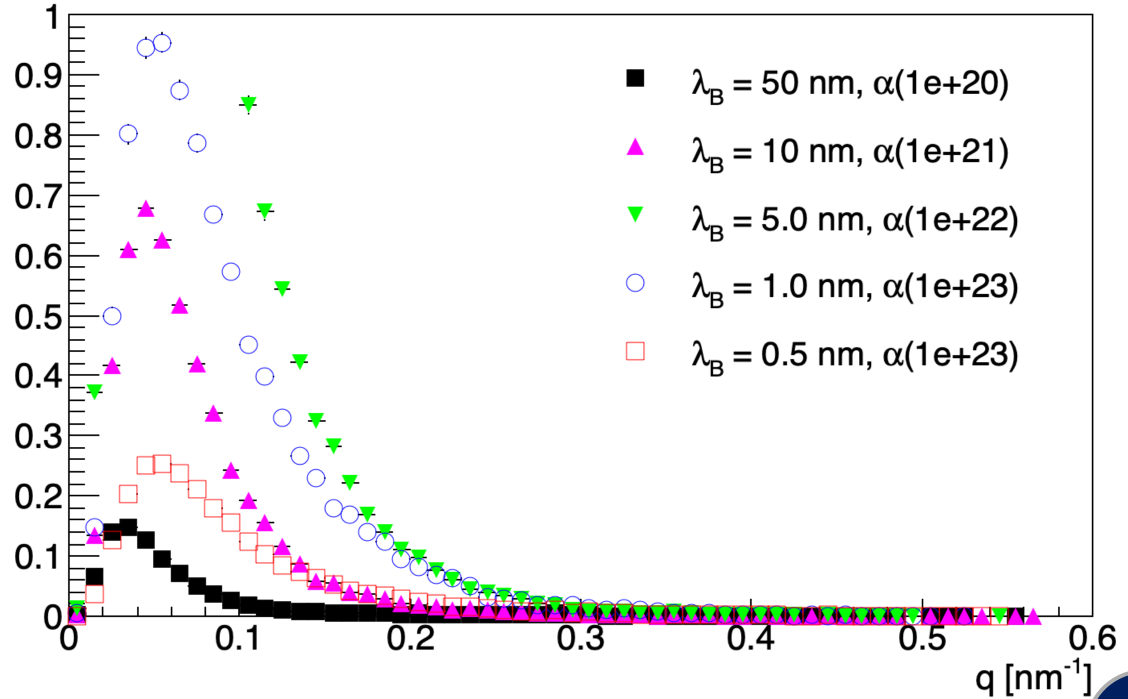

Fitting results for R(q)

This is the result of fitting by changing the Yukawa interaction length.

$\lambda_B = 50$ nm

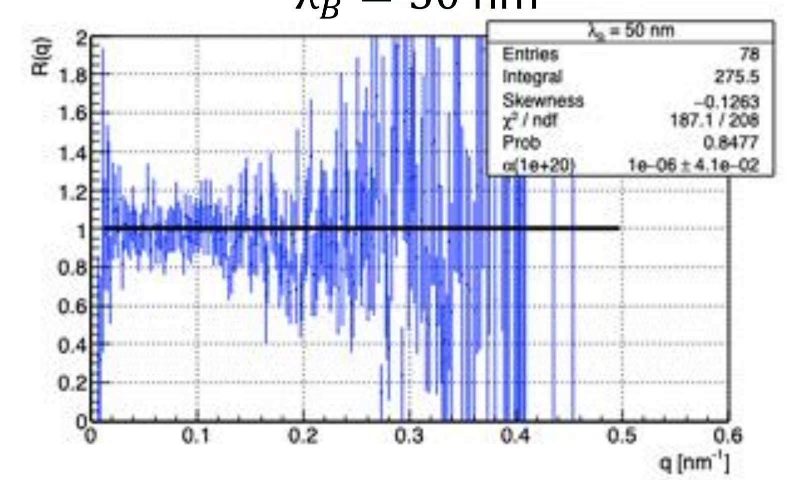

$\lambda_B = 10$ nm

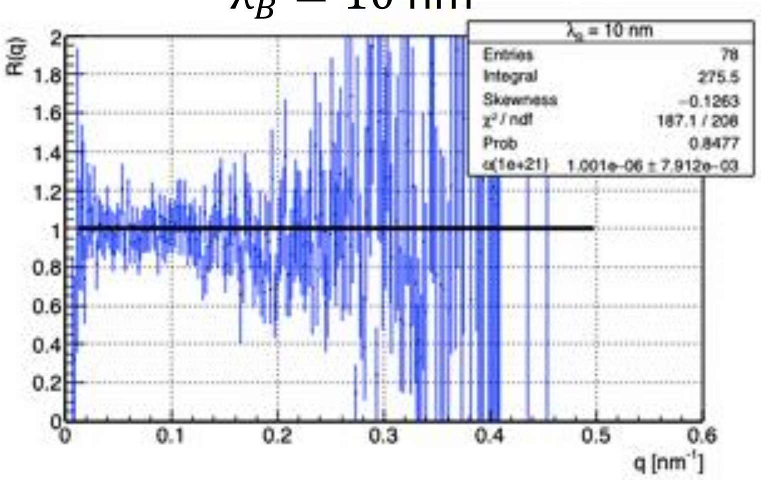

$\lambda_B = 5$ nm

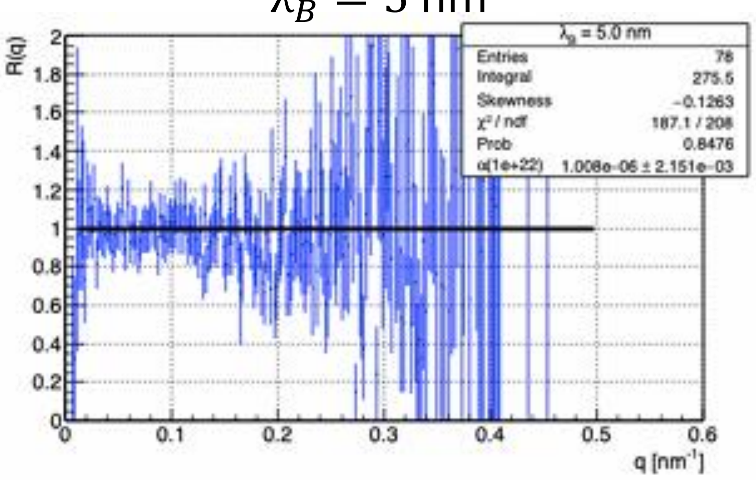

$\lambda_B = 1$ nm

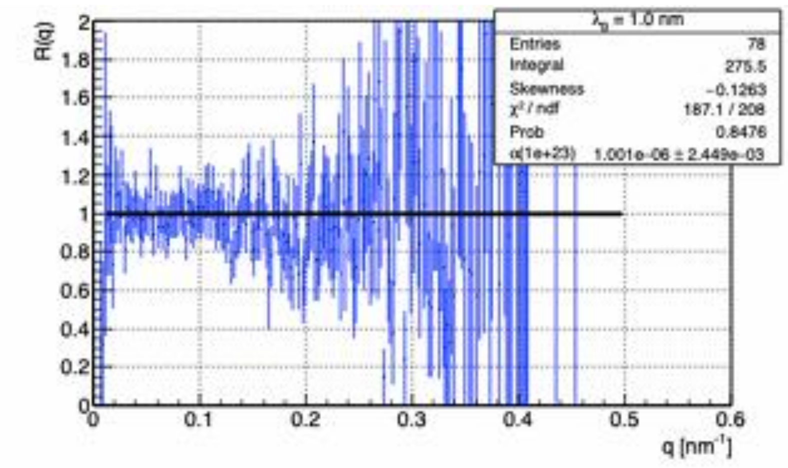

$\lambda_B = 0.5$ nm

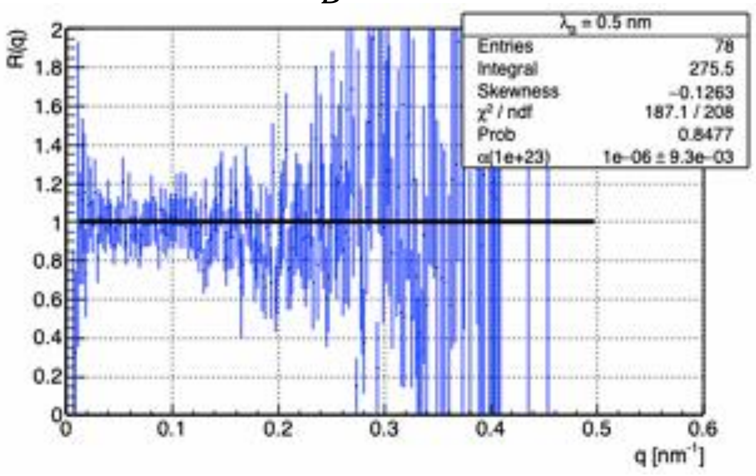

Upper limit for Yukawa interaction

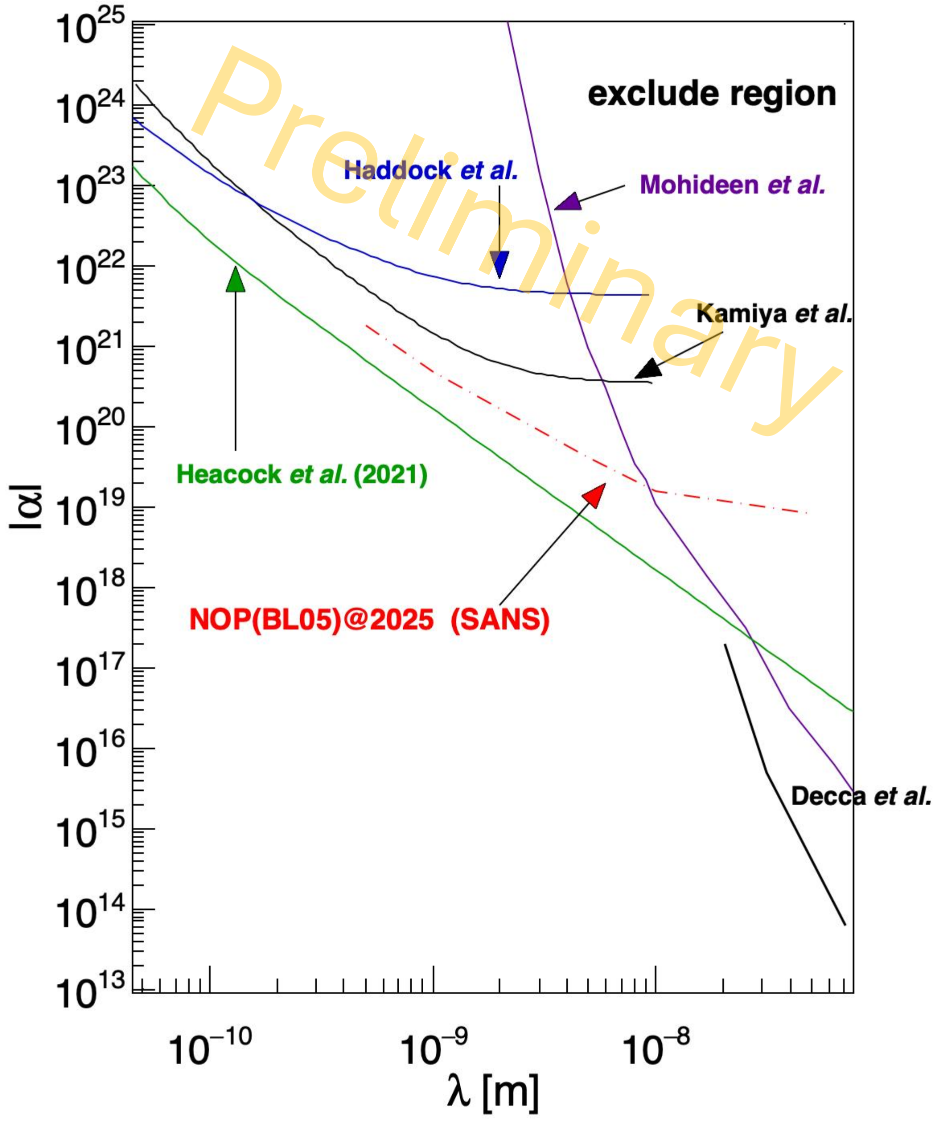

Summary

- Vanadium nanoparticles with a nuclear scattering length of 0.719±0.023 fm, close to that of natural vanadium, were created.
- The results of the SANS experiment suggest that the upper limit for the Yukawa interaction is about 2 to 3 orders of magnitude better than previous noble gas experiments.

Future plan

- Systematic errors due to density and aggregation effects will be eliminated by future SAXS measurements using the cell used in the SANS experiments.